
Molecular interactions between the constituents of small ribosomal subunit

Saurav Mallik and Sudip Kundu*

Department of Biophysics, Molecular Biology and Bioinformatics, University of Calcutta; Address: 92, APC Road, Kolkata; India; Zip: 700009

ABSTRACT

Availability of high-resolution crystal structures of ribosomal subunits of different species opens a route to investigate about molecular interactions between its constituents and stabilization strategy. Structural analysis of the small ribosomal subunit shows that primary binder proteins are mainly employed in stabilizing the folded ribosomal RNA by their high negative free energy of association, where tertiary binders mainly help to stabilize protein-protein interfaces. Secondary binders perform both the functions. Conformational changes of prokaryotic and eukaryotic ribosomal proteins due to complexation with 16S ribosomal RNA are linearly correlated with their RNA-interface area and free energy of association. The proteins having long extensions buried within ribosomal RNA have more flexible structures than those found on the subunit surface. *Thermus thermophilus* ribosomal proteins undergo high conformational changes compared to those of *Escherichia coli*, assuring structural stability at high temperature environment. The general stabilization strategy of ribosomal protein-RNA interfaces is shown, where high interface polarity ensures high surface density of Hydrogen bonds even with low base/backbone ratio. Polarity is regulated in evolutionary strategy of ribosomal proteins. Thus, the habitat environmental conditions of the two species sweep up their ribosomal protein-RNA interfaces to alter its physical parameters in order of stabilization.

1 INTRODUCTION

Ribosomes are giant ribonucleoprotein complexes that act as polymerases translating the genetic code into protein by providing the framework of positioning of the other participants in this process (Yonath, 2009; Moore, 1998). The prokaryotic ribosome consists of a larger 50S subunit and a smaller 30S subunit, of which high resolution X-ray crystallographic structures have been resolved (Wimberly *et al.* 2000; Ban *et al.* 2000; Schluenzen *et al.* 2000; Brodersen *et al.* 2002, Ben-Shem *et al.*, 2010, Korostelev *et al.*, 2006, 2009; Schuwirth *et al.*, 2005) and computationally analyzed (Noller and Baucon, 2002; Tung and Sanbonmatsu, 2004, Taylor *et al.*, 2009). Due to the functional importance of the ribosome, it is interesting to investigate about the stability of the overall complex and the interactions among its various components. The 30S subunit consists of 16S ribosomal RNA (16S rRNA) and about 21 proteins (Agalarov *et al.* 2000; Klein *et al.* 2004). The structures and positions of the proteins on 16S rRNA have been described in detail by Brodersen *et al.* 2002, Agalarov *et al.* 2000 etc. Assembly pathway of the constituents of small ribosomal subunit was analyzed much earlier. The 30S subunit has shown to be reconstituted from purified components *in vitro*, and the ordered nature of the assembly was first revealed by the elegant work of Held *et al.* 1974, known as 'Nomura Model'. An advancement of this concept is done by Mulder *et al.*, 2010 and Chen *et al.* in 2012. According to the joining with 16S rRNA during the 30S assembly pathway, the smaller subunit proteins have been divided into three classes (Held *et al.* 1974): the primary binding proteins (binds to the naked 16S rRNA: S4, S7, S8, S15 and S20), the secondary binding proteins (requires binding sites located at the RNA and primary binders to associate: S9, S12, S13, S16, S18 and S19) and the tertiary binding proteins (requires binding sites located at the RNA, primary and secondary binders to be associated: S2, S3, S5, S6, S10, S11, S14, S21 and THX).

Availability of many high-resolution crystal structures in PDB (Bernstein *et al.* 1977) has opened the possibility to analyze the stabilization strategy of 30S and 50S subunits by mutual interaction between RNA and protein components of them. In addition, the availability of crystal structures of two different species (*Escherichia coli* and *Thermus thermophilus*) being habituated in two different habitat conditions offers an opportunity to investigate whether habitat conditions have any effect on stabilization strategy of ribosomal subunits. In the current work, we have presented a detailed analysis on the molecular interactions stabilizing the 30S subunit structure. We present the relative influence of ribosomal proteins (classified according to Nomura model) in stabilization of the folded 16S rRNA at various stages of 30S assembly. We have estimated the conformational changes of the ribosomal proteins due to complexation with 16S rRNA. The linear correlation of the conformational changes of proteins on their rRNA-interface area and free energy of association has been established. A comparison of ribosomal and non-ribosomal protein-RNA interface properties establishes the unique nature of the former compared to the later. The regulation of interface polarity generates high surface density of Hydrogen bonds at the protein-rRNA interfaces, which ensures its structural stability. Interface polarity is regulated in evolutionary strategy of ribosomal proteins according to habitat conditions.

2 MATERIALS AND METHODS

Details of the materials and methods are included in the supplementary materials.

*To whom correspondence should be addressed.

2.1 Dataset

The atomic coordinate of 21 small ribosomal subunits were extracted from the PDB archive (Bernstein *et al.* 1977) on 16/05/2012. All the structures containing modified residues, full-length mRNA and tRNA, elongation factors and release factors were neglected. Eleven of our selected structures are of *Thermus thermophilus* (prokaryote); nine are of *Escherichia coli* (prokaryote) and one of *Tetrahymena thermophila* (eukaryote). A detailed description of the dataset has been included in the Supplementary Table S1. Classification of small subunit proteins are enlisted in Supplementary Table S2.

2.2 Computational Analysis

Details of the computational analysis are included in Supplementary materials.

We identified the protein-RNA and protein-protein interfaces of the 30S ribosomal subunit and several interface properties were calculated. These properties are buried surface area (BSA), free energy of interface formation (ΔG), surface density of Hydrogen-bonding (H-bonding) and van der Waals contacts at those interfaces, interface polarity, base/backbone ratio of protein-RNA H-bonding, conformational changes of the ribosomal proteins due to their interaction with 16S rRNA. In addition, we have estimated the conservation at the interfaces of ribosomal proteins.

3 RESULTS AND DISCUSSION

3.1 Influence of ribosomal proteins in 30S subunit stabilization

3.1.1 Protein-RNA interactions

We first analyze contributions of ribosomal proteins in stabilizing the final 30S structure through their interactions with 16S rRNA. The solvent accessible surface area of each protein buried against (BSA) the 16S rRNA was calculated using Surface racer program (Tsodikov *et al.*, 2002) and their free energies of association (ΔG) were calculated using PDBePISA server (Krissinel and Henrick, 2005, 2007; Krissinel 2009). The results are listed in Table-1 as average between two species (*Thermus thermophilus* and *Escherichia coli*). It is expected that the proteins having large BSAs against 16S rRNA and high negative ΔG play most important roles in stabilizing the folded 16S rRNA.

Table 1: The buried surface area (BSA) and free energy of association (ΔG) at protein-rRNA interface of ribosomal proteins are displayed. Proteins have been classified both according to Nomura model. Corresponding standard deviation values are presented in the parenthesis.

Protein Groups		Buried surface area (\AA^2)	Free energy of association (ΔG) with 16S rRNA (Kcal/mole)
Classification according to Nomura model, 1974	Primary	2091.75 (525.74)	-36.47 (12.49)
	Secondary	2337.80 (683.37)	-42.31 (16.37)
	Tertiary	1696.13 (375.94)	-29.05 (7.85)

The results show that the secondary binding proteins have the largest average BSAs and ΔG s and tertiary binders have the lowest. Primary binders associate with 16S rRNA with BSA and ΔG values slightly less than secondary binders. The average BSA of the primary binding proteins is 2091.75 \AA^2 and that for secondary binders is 2337.80 \AA^2 . The free energies of association of the primary and secondary binders are -36.47 Kcal/mole and -42.31 Kcal/mole, respectively. The comparatively much lower average BSA (1696.13 \AA^2) and ΔG (-29.05 Kcal/mole) of tertiary binding proteins with 16S rRNA indicate that these proteins are less important in stabilization of the folded 16S rRNA compared to primary and secondary binders. The BSA and ΔG values of the individual proteins for both *E. coli* and *T. thermophilus* have been enlisted in Supplementary Table S3 and S4, respectively.

The statistical significance test (Supplementary Table S5) shows that the primary and secondary binding proteins are originated from the same populations. On the other hand, the difference of this population from tertiary binders is marginally significant ($p=0.03$). In addition, we generate a hierarchical cluster (using UPGMA method: Gronau and Moran, 2007) of proteins using their BSAs. Four distinct groups (Supplementary Figure F1) were identified; and among them, two groups (Group-1 and Group-2) with high BSAs and high negative ΔG of associations (statistically significantly different from other groups) consist of three primary (S4, S17 and S20) and three secondary (S9, S12 and S16) binders proteins (Table S6). Thus, the primary and secondary binders play more important role in stabilizing protein-rRNA complexed structure, compared to tertiary binders.

3.1.2 Protein-protein interactions

Next, we study how the ribosomal proteins mutually interact to reduce the overall ΔG value of the 30S subunit structure and contribute further to its stabilization. The results are included in Table 2. The corresponding values for *T. thermophilus* and *E. coli* are presented in Supplementary Table S7.

Table 2: The protein-protein interface properties of *T. thermophilus* and *E. coli* ribosomes; abbreviations used in this table: $\sigma(H)$ =number of H-bonds per 100\AA^2 buried surface area (interface area), $\sigma(v)$ = number of van der Waals contacts per 100\AA^2 buried surface area, ΔG = free energy of interface formation.

Protein-protein interactions classified according to association		Interface Properties
Classification	Protein-protein interfaces	
Primary-Primary	S8-S17	$\sigma(H)$ = 2.60 $\sigma(v)$ = 18.00 ΔG = -0.70
Primary-Secondary	S7-S9, S8-S12, S12-S17	$\sigma(H)$ = 0.30 $\sigma(v)$ = 1.93 ΔG = -2.10
Primary-Tertiary	S2-S8, S3-S4, S4-S5, S5-S8, S7-S11	$\sigma(H)$ = 1.17 $\sigma(v)$ = 10.63 ΔG = -0.76
Secondary-Secondary	S9-S10, S9-S13, S13-S19	$\sigma(H)$ = 0.95 $\sigma(v)$ = 12.65 ΔG = -1.17
Secondary-Tertiary	S6-S18, S9-S14, S11-S18, S14-S19, S18-S21	$\sigma(H)$ = 10.63 $\sigma(v)$ = 46.45 ΔG = -2.49
Tertiary-Tertiary	S2-S3, S2-S5, S3-S5, S3-S10, S3-S14, S10-S14, S11-S21	$\sigma(H)$ = 1.80 $\sigma(v)$ = 14.68 ΔG = -4.23

An average secondary-tertiary interface is associated with -2.49 Kcal/mole free energy, where tertiary-tertiary interfaces are associated with average -3.08 Kcal/mole free energy. Thus, they form very stable interfaces among themselves. The secondary-secondary interfaces are also very stable (with average -1.17 Kcal/mole free energy of association). However, primary-primary and primary-tertiary interfaces have lower values of ΔG in comparison to the other interactions. Interestingly, while the tertiary binders have a lower ΔG of interface formation with primary binders (-0.76 Kcal/mole); the secondary binders have higher values of ΔG of interface formation with primary binders (-2.10 Kcal/mole). The average values of surface densities of van der Waals contacts of tertiary binders (secondary-tertiary, primary-tertiary and tertiary-tertiary) are higher than those of other interfaces. The tertiary binders do also have the highest surface density of hydrogen bonds with the primary binders.

3.1.3 The roles of proteins at various stages of 30S subunit protein-RNA assembly

In case of protein-RNA interactions of 30S subunit, we observe that the primary and secondary binding proteins have higher negative free energies of association with the 16S rRNA (Table 1). Table 2 depicts that the average solvent free energy changes due to protein-protein associations are remarkably high for tertiary-tertiary and secondary-tertiary interactions compared to the others. Thus, we find that primary binders significantly stabilize the protein-rRNA interfaces and tertiary binders mainly stabilize the protein-protein interfaces of 30S subunit. Secondary binders play both the roles significantly.

The above results clearly indicate the possible underlying biophysical principles during the ribosomal assembly. In the initial states of 30S assembly process, the proteins bind to the naked 16S rRNA, which has a very high folding free energy (isolated structure has about +4000 Kcal/mole solvation free energy for *E. coli*, calculated using PDBePISA server). Therefore, the unfolding of naked 16S rRNA in the initial stages of assembly is highly favorable. The primary binding proteins, which associate first with 16S rRNA, play an important role in stabilizing the folded 16S rRNA initially and prevent the unfolding. The secondary binders then associate and contribute further to the rRNA stabilization. In addition, they form stabilized protein-protein interfaces with primary and tertiary binders that cause the 30S ribosome structure intact. Finally, tertiary binders, with their high free energies of protein-protein associations and high inter surface densities of H-bonds and van der Waals contacts provide the final stability to the 30S ribosomal complex.

3.2 Conformational changes of 30S subunit proteins upon complexation with 16S rRNA

Here, we study the conformational changes of the ribosomal proteins due to their interaction with the 16S rRNA and its dependency on other physico-chemical properties.

3.2.1 Protein conformational changes

Most of the ribosomal proteins have several extended domains buried in RNA; being isolated from the subunit, they do not contain these extensions (Brodersen *et al.*, 2002). Thus, the usual structural alignment method (comparison of un-complexed and complexed form) is not a suitable one in this case to measure the conformational changes due to complexation. Therefore, we have used another algorithm, (Marsh and Teichmann, 2011), which can predict the probable conformational change occurring in a protein monomer due to complexation with its partner. (see Supplementary Materials, section 1.4). Conformational changes are expressed in terms of Root Mean Square Distance (RMSD) between the aligned uncomplexed and complexed structures. The predicted RMSD values between complexed and uncomplexed states of the ribosomal proteins are presented in Table 2. The predicted RMSD values vary in a wide range for both the species. Below we explain the significance of conformational changes of individual proteins.

Table 3: The predicted conformational changes of the ribosomal proteins due to their complexation within the 30S ribosomal subunit are listed here. Conformational changes are expressed in terms of Root Mean Square Distance (RMSD) between the aligned uncomplexed and complexed structures.

Ribosomal proteins	Predicted RMSD between complexed and uncomplexed states (Å)	
	<i>T. thermophilus</i>	<i>E. coli</i>
S2	2.98	2.63
S3	5.61	5.01
S4	4.71	3.66
S5	2.99	2.93
S6	3.89	1.67
S7	7.69	5.70
S8	3.07	2.59
S9	6.56	5.00
S10	9.12	7.57
S11	5.56	4.88
S12	18.76	11.14
S13	14.25	8.10
S14	19.19	17.50
S15	5.78	3.90
S16	2.25	3.04
S17	9.79	5.08
S18	5.04	3.31
S19	6.83	4.80
S20	8.94	5.72
S21	-	32.26
THX	4.30	-

Brodersen *et al.* (2002) showed that S2, S4, S5 and S8 proteins have large globular domains which are found on the surface of 30S subunit; they usually have small extended regions buried within 16S rRNA. On the other hand, S12, S13, S14, S17 and S19 have comparatively long rRNA buried extended regions. Authors hypothesized that proteins having long RNA-buried extensions assist 16S rRNA folding. Thus, it follows that such proteins should undergo high conformational changes during 16S rRNA folding and should have more flexible structures compared to the proteins found on the surface of 30S subunit.

Following the work of Marsh and Teichmann, we predict the flexibilities of small subunit proteins (Supplementary Table S8a) and clustered them (UPGMA method) into three groups in increasing order: (Group-A) S2, S5, S6, S8, S16, (Group-B) S3, S4, S7, S9, S11, S15, S19; (Group-C) S10, S17, S18, S20; (Group-D) S12, S13, S14. Group-A and B proteins are found on 16S rRNA surface. They have small RNA buried extensions, rigid structures and undergo small conformational changes upon interaction with 16S rRNA (average RMSD on both species are 2.80 and 5.14 respectively). Group-C proteins have intermediate structural flexibility, comparatively longer RNA buried extensions; they undergo intermediate structural changes (average RMSD=7.45). Group-D proteins have long RNA buried extensions and highly flexible structures which experience large structural changes (average RMSD=14.82). Difference between Group-A and B ($p(A-B)=0.001$) and Group-B and C ($p(B-C)=0.004$) are significant. Group-D is marginally different from every other group ($p(C-D)=0.05$; $p(A-D)=0.035$; $p(B-D)=0.012$). Group-A and C are also marginally different ($p(A-C)=0.015$).

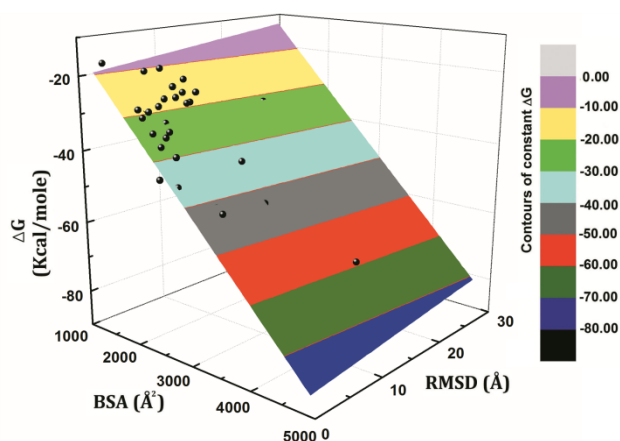


Figure-1: The 3D surface plot for ΔG , RMSD and BSA is shown here. The surface is presented as 3D colormap, with projection on the BSA-RMSD plane shows the contours of constant ΔG . Black dots represent the data points (not all are visible as some data points are beneath the surface). This plot is generated by Origin data analysis and graphic workspace (37), using the ribosomal protein-RNA association data from two bacteria (*E. coli* and *T. thermophilus*) and one eukaryotic species (*T. thermophila*).

It also appears from Marsh and Teichmann's work that S12 and S14 (for both *E. coli* and *T. thermophilus*) are likely to be intrinsically disordered, which also follows from predictions of DisEMBL server (Linding *et al.*, 2003). Marsh and Teichmann showed (for protein-protein interactions) that upon complex formation, intrinsically disordered protein monomers undergo high structural changes. This might entail the fact that disordered proteins often show disorder-to-order transitions upon complex formation (Wright, 1999; Fink, 2005; Dunker *et al.*, 2002; Radivojac *et al.*, 2004). The high conformational change of S12 and S14 during its assembly with 16S rRNA might be the result of such a disorder-to-order transition event. Another interesting fact is that, most of the proteins of *T. thermophilus* experience higher conformational changes compared to those of *E. coli*. Implication of this is discussed in section 3.3.

3.2.2 Protein conformational changes depend on BSA and ΔG of protein-rRNA interfaces

Next, we have tried to explore whether there exist any relationship between conformational changes, and the strength of protein-rRNA interaction, represented by ΔG of association and BSA. Earlier works (Janin *et al.*, 1988; Lo Conte *et al.*, 1999) have shown in case of protein-protein interactions, the conformational changes of the monomers depend on their interface area. However, in ribosomal protein-RNA interactions (using data for the three species together), we observe a very low value of linear correlation coefficient ($r=0.35$, $R\text{-square}=0.13$) between conformational change (RMSD) and BSA. We also observe a poor linear fitting of RMSD and ΔG of association ($r=0.27$, $R\text{-square}=0.09$). Interestingly, the three parameters, all-together, correlate very well with each other in a linear equation ($r=0.93$ and $R\text{-square}=0.86$), defining a plane surface in a three-dimensional space. The linear equation is shown in the following:

$$\Delta G = a + b(\text{BSA}) + c(\text{RMSD}) \quad (1)$$

Here a , b and c are the fitting constants. This very equation is observed in both the bacterial species (*T. thermophilus* and *E. coli*) and is followed in an eukaryotic ribosome (*Tetrahymena thermophila*) as well. However, the values of the coefficients, a , b and c are species specific. In Supplementary Table S8b, the surface fitting statistics along with the values of these three constants for the three species have been included. The high correlation among the three parameters entails that the conformational changes of the ribosomal proteins are not

solely dependent on the BSA or ΔG of association. In fact, both the physical parameters jointly determine the conformational changes of the ribosomal proteins.

The 3D surface plot using the average BSA, RMSD and ΔG values of the three species (*T. thermophilus*, *E. coli* and *T. thermophila*) is presented in Figure-1. It follows from Equation-1 that proteins with high negative ΔG of association with 16S rRNA and large interface areas experience more conformational changes upon interaction compared to those having smaller interfaces and low ΔG of association. Nevertheless, when we modify our data taking into account protein-protein interactions, this linear correlation becomes very poor. This probably indicates the fact that major structural changes of the ribosomal proteins occur due to complexation with the 16S rRNA only.

3.3 Generalized Stabilization Strategy of 30S Subunits in both Bacterial Species

While studying the *E. coli* and *T. thermophilus* separately, we observe that the same strategy is followed by both the species to stabilize their 30S subunit assembly. However, there exists difference in the corresponding values of interface parameters of two species, which can be correlated with the habitat conditions they live in. Our results are discussed in the following.

3.3.1 Primary and Secondary Binder play major roles in stabilizing 16S rRNA structure: We list below the free energies of 16S rRNA-protein associations. The values for primary binders are -39.51 Kcal/mole and -35.84 Kcal/mole for *T. thermophilus* and *E. coli*, respectively. Those for secondary binders are -40.09 Kcal/mole and -41.00 Kcal/mole. The tertiary binders have -25.99 Kcal/mole and -29.32 Kcal/mole. Thus, we observe that the primary and secondary binders, through their large negative free energy changes provide a major structural stability to the 16S rRNA-protein complex in both the species.

However, the primary binders of *T. thermophilus* associate with 16S rRNA with higher BSA and higher ΔG compared to those of *E. coli*. This might entail the fact that at its high temperature habitat *T. thermophilus* 16S rRNA faces higher probability of unfolding/denaturation compared to that of *E. coli* at the earliest stages of 30S subunit assembly. Therefore, *T. thermophilus* requires proteins with higher ΔG of association to prevent the unfolding of 16S rRNA at the initial stages of 30S subunit protein-rRNA assembly, compared to those of *E. coli*. We do also observe that the BSAs of primary and secondary binders of the individual species are higher than those of tertiary binders (Table-1).

3.3.2 Secondary and Tertiary binders form stable protein-protein interfaces: In case of ribosomal protein-protein interactions, we observe that secondary and tertiary binders form highly stabilized interfaces as they interact mutually or with themselves. This general trend shows some variations in the individual species as well. An average secondary-tertiary interface is associated with -1.37 Kcal/mole free energy in *T. thermophilus* and -1.22 Kcal/mole free energy in *E. coli*. Primary-secondary interfaces have average -2.63 Kcal/mole free energy in *T. thermophilus* and -1.57 Kcal/mole free energy in *E. coli* (Supplementary Table S7). The high conformational changes of *T. thermophilus* proteins due to complexation with 16S rRNA follows from their high BSA and high ΔG of association compared to those of *E. coli*.

3.3.3 Ribosomal protein-RNA interfaces compensate low base/backbone ratio by high interface polarity: The double stranded A-form structure of the 16S rRNA causes most of its bases unavailable for proteins to form H-bonds, since they already have been used up for base pair formation. Therefore, a major selectivity is accepted by the ribosomal proteins to form H-bonds with the sugar-phosphate backbone of RNA. Jones *et al.* (2001) reported for non-ribosomal protein-RNA interactions that the interface H-bonding between proteins and RNA follows equal selection for RNA bases and backbone, thereby resulting base/backbone ratio to be unity. The base/backbone ratio of number of Hydrogen bonds formed between RNA and proteins gives us a demonstration of the major selection of RNA backbone for H-bond formation by the ribosomal proteins.

A comparison of the Hydrogen bond density of non-ribosomal (Jones *et al.*, 2001) and ribosomal protein-RNA interfaces (Table-4) shows that the later is higher than the former, with the special features of the ribosomal proteins having very low base/backbone ratio and high interface polarity. Non-ribosomal protein-RNA interface polarity was calculated to be 45.7% by Jones *et al.*. In addition, average ribosomal protein-RNA interface maintains 1.87 H-bonds per 100 Å² BSA, which is significantly higher than that of non-ribosomal (1.2 H-bonds per 100 Å² BSA). Having most of the H-bond donor and acceptor groups of rRNA bases being used up for base pair formation, the ribosomal protein-RNA interfaces face the availability of lesser number of H-bonding partners from nucleic acid bases (mainly backbone is available), compared to the non-ribosomal proteins (bases are available in higher propensity) per unit buried surface area. However, a high protein-rRNA interface polarity (Table S12) causes a relative increment of the surface density of available hydrogen bonding partners. Ribosome protein-rRNA interfaces have higher number of H-bonds among positive charged residues of proteins and negatively charged backbone of rRNA. Thus, an H-bonding surface density higher than the non-ribosomal protein-RNA interfaces is maintained in protein-rRNA interfaces even with a low base/backbone ratio.

The observed lower base/backbone ratio refers to the fact that the ribosomal H-bonding formation favors the backbone of RNA compared to the nucleotide bases and our result is consistent with a very recent observation (Gupta and Gribskov, 2011). Here, we extend their work by observing that *T. thermophilus* maintains a lower base/backbone ratio compared to *E. coli*. The *T. thermophilus* bacteria, being a habitat of high temperature environment, needs stronger protein-RNA contacts for gaining high stabilization and keep its ribosome structure intact, compared to *E. coli*. In addition to it, *T. thermophilus* faces a problem of low base/backbone ratio (0.75) compared to that of *E. coli* (0.83). Thus, for generating a high surface density of Hydrogen bonds at the protein-RNA interfaces, it has evolved with a high interface polarity.

Table-4: The comparison of *T. thermophilus* and *E. coli* and of non-ribosomal and ribosomal protein-RNA interface properties is shown in this table. See Supplementary section 1.2 and 1.3 for definitions of parameters. Surface density of H-bonding is expressed as number of H-bonds per 100 Å² BSA.

Protein-RNA interface parameters	<i>T. thermophilus</i> values	<i>E. coli</i> values	Average values for protein-rRNA interfaces	Values for Non-ribosomal protein-RNA interfaces [33]
Base/Backbone ratio	0.75	0.83	0.79	1.00
Interface Polarity	64.13%	62.5%	63.34%	45.7%
Surface density of H-bonding	1.94	1.79	1.87	1.20

3.3.4 Polarity is conserved in evolutionary strategy of ribosomal proteins: These pictures suggest that the interface polarity is adjusted in the evolutionary strategy of ribosome to adopt with the habitat conditions and keep structures intact. On the other hand, a comparison of ribosomal and non-ribosomal protein-RNA interfaces shows that due to structural constraints the former had to keep high interface polarity to assure highly stabilized protein-rRNA interfaces. High interface polarity can be maintained in two ways: one, by conserving interface residues (interface residues are mostly positively charged amino acids) and two, by replacing the interface residues by those of same charge. We have confirmed both these evolutionary strategy in Table S9a and Table S9b. The ‘residue conservation factor’ and ‘charge conservation factor’ values of ribosomal protein-RNA and protein-protein interfaces being greater than unity confirms our arguments (see materials and methods for definition of these two parameters). Thus, the necessity for maintenance of high polar interface (which seems to be a general stabilization strategy for protein-rRNA interfaces) also modulates the evolutionary trend of ribosomal proteins.

3.3.5 Overall comparison between the stabilization strategy of *T. thermophilus* and *E. coli*: From the previous results of individual species, we find an interesting general trend (with few exceptions). The proteins of *T. thermophilus* interact with 16S rRNA with higher BSA and higher ΔG than those of *E. coli* and consequently experience higher conformational changes. In addition, the protein-RNA interfaces of *T. thermophilus* are rich in hydrogen bonds and van der Waals contacts compared to those of the *E. coli*. This general trend can be explained by the fact that *E. coli* is habituated to live in normal conditions (room temperature) and *T. thermophilus* is habituated in extreme conditions (high temperature). *T. thermophilus*, even at high temperature, probably maintains the structural stability of its 30S ribosomal subunit through higher negative free energy of protein-rRNA association, H-bonding, and van der Waals contact; and the higher conformational change of the ribosomal proteins helps to attain these.

4 CONCLUSIONS

The dataset of 21 small ribosomal subunit structures is the largest dataset analyzed in this kind of analysis to date. Our work provides a number of new insights to the structure and stabilization of the 30S ribosomal complex. At the initial stages of the ribosomal association pathway, primary binder proteins provide high free energy of association and prevent its unfolding. Consequently, secondary binders join the subunit and form highly stabilized interfaces both with the 16S rRNA and primary binders; and generate potential site of interaction with the tertiary binder proteins. Tertiary binders finalize the assembled 30S structure and they mainly form stabilized protein-protein interfaces.

We do not only predict the conformational changes of the ribosomal proteins upon interaction with 16S rRNA, further linearly correlate them with the BSA and ΔG values of association. Conformational changes of proteins have been explained using their structural properties and binding strategy with 16S rRNA. We have identified the flexible and disordered proteins of 30S subunit. This linear relationship is

confirmed in two bacterial and a eukaryotic species. We propose that this linearity might be a general rule of ribosomal protein-RNA assembly and will be followed in any ribosome of any species.

Further, we show that interface polarity is regulated in evolutionary strategy of ribosomal proteins. High polarity ensures high surface density of H-bonds and thereby provides structural stability to the 30S subunit. Therefore, the environmental conditions sweep up the interfaces of the ribosome to alter its physical states.

ACKNOWLEDGEMENTS

The authors acknowledge the computational facility of DIC and Department of Biophysics, Molecular Biology and Bioinformatics, University of Calcutta. This research work is not funded by any authority; the authors performed it on their personal interests.

SUPPLEMENTARY MATERIALS

Supplementary Materials and Methods (section 1), Tables S1-S12, Figures F1, Discussion (Section 2) and References (section-3) are available online.

REFERENCES

- Agalarov, S.C., Prasad, G.S., Funke, P.M., Stout, C.D., Williamson, J.R. (2000). Structure of S15, S6, S18-rRNA Complex: Assembly of the 30S ribosome central domain. *Science*, 288, 5463, 107-112.
- Ban, N., Nissen, P., Hansen, J., Moore, P.B., and Steitz, T.A. (2000). The complete atomic structure of the large ribosomal subunit at 2.4Å resolution. *Science*, 289, 905-920.
- Ben-Shem, A., Jenner, L., Yusupova, G., Yusupov, M. (2010). Crystal structure of the eukaryotic ribosome, *Science*;330(6008):1203-9.
- Bernstein, F.C., Koetzle, T.F., Williams, G.J., Meyer, E.E. (Jr.), Brice, M.D., Rodgers, J.R., Kennard, O., Shimanouchi, T., Tasumi, M., (1977). The Protein Data Bank: A Computer-based Archival File For Macromolecular Structures, *J. Mol. Biol.*, 112, 535-542.
- Brodersen, D. E., Clemons, W. M., Jr, Carter, A. P., Wimberly, B. T. and Ramakrishnan, V. (2002). Crystal structure of the 30S ribosomal subunit from *Thermus thermo-philus*: structure of the proteins and their interactions with 16 S RNA. *J. Mol. Biol.* 316, 725–768.
- Chen, K., Eargle, J., Lai, J., Kim, H., Abeyvirigunawardena, S., Mayerle, M., Woodson, S., Ha, T., Luthey-Schulten Z. (2012). Assembly of the five-way junction in the ribosomal small subunit using hybrid MD-Go simulations, *J Phys Chem B.*;116(23):6819-31.
- Dunker, A.K., Brown, C.J., Lawson, J.D., Iakoucheva, L.M., Obradovic, Z. (2002). Intrinsic disorder and protein function. *Biochemistry* 41: 6573–6582.
- Fink, A.L. (2005). Natively unfolded proteins. *Curr Opin Struct Biol* 15: 35–41.
- Gupta, A., Gribskov, M. (2011). The role of RNA sequence and structure in RNA-protein interactions. *J. Mol. Biol.* 409, 574–587.
- Held, W.A., Ballou, B., Mizushima, S., Nomura, M. (1974). Assembly mapping of 30S ribosomal proteins from *Escherichia coli*. *J. Biol. Chem.* 249, 3103-3111.
- Janin, J., Miller, S., Chothia, C. (1988). Surface, subunit interfaces and interior of oligomeric proteins. *J. Mol. Biol.*; 204:155–164.
- Jones, S., Daley, D.T.A., Luscombe, N.M., Berman, H.M., Thornton, J.M. (2001). Protein-RNA interactions: a structural analysis. *Nucleic Acid research*, vol. 29, no. 4, 943-954.
- Klein, D.J., Moore, P.B., Steitz, T.A. (2004). The role of Ribosomal Proteins in the Structure Assembly and Evolution of the large Ribosomal Subunit. *J. Mol. Biol.* 340, 141-177.
- Korostelev, A., Laurberg, M., and Noller, H.F. (2009). Multistart simulated annealing refinement of the crystal structure of the 70S ribosome, *Proc Natl Acad Sci USA* 106:18195-18200.
- Korostelev, A., Trakhanov, S., Lauerberg, M., and Noller, H.F. (2006). Crystal Structure of a 70S Ribosome-tRNA Complex Reveals Functional Interactions and Rearrangements. *Cell.* 126:1065-1077.
- Krissinel, E. (2009). Crystal contacts as nature's docking solutions. *J Comput Chem.* 2010 Jan 15;31(1):133-43.; DOI 10.1002/jcc.21303.
- Krissinel, E. B., Winn, M. D., Ballard, C. C., Ashton, A. W., Patel, P., Potterton, E. A., McNicholas, S. J., Cowtan, K. D., Emsley, P. (2004). The new CCP4 coordinate library as a toolkit for the design of coordinate related applications in protein crystallography. *Acta Cryst.* D60, 2250–2255.

- Krissinel, E., Henrick, K. (2004). Secondary structure matching (SSM), a new tool for fast protein structure alignment in three dimensions. *Acta Cryst.* D60, 2256-2268.
- Linding, R., Jensen, L.J., Diella, F., Bork, P., Gibson, T.J., Russell, R.B. (2003). Protein disorder prediction: implications for structural proteomics, *Structure*;11(11):1453-9
- Lo Conte, L., Chothia, C., Janin, J. (1999). The atomic structure of protein-protein recognition sites. *J. Mol. Biol.*; 285:2177-2198.
- Marsh, J.A., Teichmann, S.A. (2011). Protein solvent accessible surface area predicts protein conformational changes upon binding. *Structure*. 19, 859-867.
- Moore, P.B. (1998). The three dimensional structure of the ribosome and its components. *Annu. Rev. Biophys. Biomol. Struct.*, 27, 35-58.
- Mulder, A. M., Yoshioka, C., Beck, A. H., Bunner, A. E., Milligan, R. A., Potter, C. S., Carragher, B., Williamson, J. R. (2010). Visualizing ribosome biogenesis: parallel assembly pathways for the 30S subunit, *Science*;330(6004):673-7.
- Noller, H. F. and A. Baucom (2002). Structure of the 70 S ribosome: implications for movement. *Biochem Soc Trans* 30(6): 1159-61.
- OriginPro 8 SR0, v8.0724 (B724). Copyright © 1991-2007 OriginLab Corporation.
- Radojic, P., Obradovic, Z., Smith, D. K., Zhu, G., Vucetic, S., Brown, C. J., Lawson, J. D., Dunker, A. K. (2004). Protein flexibility and intrinsic disorder, *Protein Sci.*;13(1):71-80.
- Schluenzen, F., Tocilj, A., Zarivach, R., Harms, J., Gluehmann, M., Janell, D., Bashan, A., Bartels, H., Agmon, I., Franceschi, F., and Yonath, A. (2000). Structure of functionally activated small ribosomal subunit at 3.3 angstroms resolution. *Cell*, 102, 615-623.
- Schuwirth, B. S., Borovinskaya, M. A., Hau, C. W., Zhang, W, Vila-Sanjurjo, A., Holton, J. M., Cate, J. H. (2005). Structures of the bacterial ribosome at 3.5 A resolution, *Science*;310(5749):827-34.
- Taylor, D. J., Devkota, B., Huang, A. D., Topf, M., Narayanan, E., Sali, A., Harvey, S. C., Frank, J. (2009). Comprehensive molecular structure of the eukaryotic ribosome, *Structure*;17(12):1591-604.
- Tsodikov, O. V., Record, M. T. Jr. and Sergeev, Y. V. (2002). A novel computer program for fast exact calculation of accessible and molecular surface areas and average surface curvature. *J. Comput. Chem.*, 23, 600-609.
- Tung, C. S., Sanbonmatsu, K. Y. (2004). Atomic model of the *Thermus thermophilus* 70S ribosome developed in silico, *Biophys J.*;87(4):2714-22.
- Wimberley, B.T., Brodersen, D.E., Clemons, W.M. (Jr), Morgan-Warren, J.R., Carter, A.P., Vornrhein, C., Hartsch, T., Ramakrishnan, V. (2000). Structure of the 30S ribosomal subunit. *Nature*, 407, 327-339.
- Wright, P.E., Dyson, H.J. (1999) Intrinsically unstructured proteins: re-assessing the protein structure-function paradigm. *J Mol Biol* 293: 321-331.
- Yonath, A. (2009). Large facilities and the evolving ribosome, the cellular machine for genetic code translation. *J. R. Soc. Interface*, 6, S575-S585.

SUPPLEMENTARY MATERIALS

1. MATERIALS AND METHODS (in details)

1.1 DATASET

We collected a large set of 21 ribosomal complexes from PDB on 16/05/2012. Eleven of them are *Thermus thermophilus* (bacteria), nine from *Escherichia coli* (bacteria), and one from *Tetrahymena thermophila* (eukaryote). The PDB codes of these complexes with additional informations and citations are summarized in Table S1. We neglected all the structures containing modified residues, full length tRNA, mRNA, elongation factors and release factors. Except them, these 15 structures were collected from the whole PDB archive. Structures with ≥ 4.0 Å resolution are also disregarded. However, 1XNQ and 1IBK contains small fragments of mRNA (3-4 nucleotides only). Unique structures containing only ribosomal RNA and ribosomal proteins (there may be antibiotics and other small molecules bound) were selected for our analysis. Yeast ribosomal complexes are available in PDB, but as we will explain in the following, detectable protein-rRNA interfaces were not identified in them. Therefore, we used the only available *Tetrahymena thermophila* ribosomal structure, in spite of presence of modified residues in it.

Table S1. The Dataset of 21 ribosomal complexes collected from PDB.

Organism	PDB-ID	Resolution (Å)	Citation
<i>Thermus thermophilus</i>	1FJG	3.00	Carter, A.P., Clemons Jr., W.M., Brodersen, D.E., Morgan-Warren, R.J., Wimberly, B.T., Ramakrishnan, V. (2000) Nature 407 : 340-348
	1N36	3.65	Ogle, J.M., Murphy IV, F.V., Tarry, M.J., Ramakrishnan, V. (2002) , Cell(Cambridge,Mass.) 111 : 721-732
	1XNQ	3.05	Murphy, F.V., Ramakrishnan, V. (2004) Nat.Struct.Mol.Biol. 11 : 1251-1252
	2E5L	3.30	Kaminishi, T., Wilson, D.N., Takemoto, C., Harms, J.M., Kawazoe, M., Schlutzen, F., Hanawa-Suetsugu, K., Shirouzu, M., Fucini, P., Yokoyama, S. (2007) Structure 15 : 289-297
	2F4V	3.80	Murray, J.B., Meroueh, S.O., Russell, R.J., Lentzen, G., Haddad, J., Mobashery, S. (2006) Chem.Biol. 13 : 129-138
	1IBK	3.31	Ogle, J.M., Brodersen, D.E., Clemons Jr., W.M., Tarry, M.J., Carter, A.P., Ramakrishnan, V. (2001) Science 292 : 897-902
	2ZM6	3.30	Kaminishi, T., Wang, H., Kawazoe, M., Ishii, R., Hanawa-Suetsugu, K., Nomura, M., Takemoto, C., Shirouzu, M., Paola, F., Yokoyama, S. (to be published)
	3OGE	3.00	Bulkley, D., Innis, C.A., Blaha, G., Steitz, T.A. (2010). Revisiting the structures of several antibiotics bound to the bacterial ribosome. Proc.Natl.Acad.Sci.USA 107 : 17158-17163
	3UXT	3.20	Bulkley, D., Johnson, F., Steitz, T.A., (2012) J.Mol.Biol. 416 : 571-578
	3OHC	3.00	Bulkley, D., Innis, C.A., Blaha, G., Steitz, T.A., (2010) Proc.Natl.Acad.Sci.USA 107 : 17158-17163
	2HHH	3.35	Schlutzen, F., Takemoto, C., Wilson, D.N., Kaminishi, T., Harms, J.M., Hanawa-Suetsugu, K., Szaflarski, W., Kawazoe, M., Shirouzu, M., Nierhaus, K.H., Yokoyama, S., Fucini, P., (2006) Nat.Struct.Mol.Biol. 13 : 871-878
<i>Escherichia coli</i>	2AVY	3.46	Schuwirth, B.S., Borovinskaya, M.A., Hau, C.W., Zhang, W., Vila-Sanjurjo, A., Holton, J.M., Cate, J.H. (2005) Science 310 : 827-834
	3OAQ	3.25	Dunkle, J.A., Xiong, L., Mankin, A.S., Cate, J.H. (2010) Proc.Natl.Acad.Sci.USA 107 : 17152-17157
	2QAN	3.21	Borovinskaya, M.A., Pai, R.D., Zhang, W., Schuwirth, B.S., Holton, J.M., Hirokawa, G., Kaji, H., Kaji, A., Cate, J.H. (2007) Nat.Struct.Mol.Biol. 14 : 727-732
	3DF1	3.50	Borovinskaya, M.A., Shoji, S., Fredrick, K., Cate, J.H.D. (2008) Rna 14 : 1590-1599
	2VHO	3.00	Bingel-Erlenmeyer, R., Kohler, R., Kramer, G., Sandikci, A., Antolic, S., Maier, T., Schaffitzel, C., Wiedmann, B., Bukau, B., Ban, N. (2008) Nature 452 : 108
	2QP0	3.50	Borovinskaya, M.A., Shoji, S., Holton, J.M., Fredrick, K., Cate, J.H. (2007). A steric

			block in translation caused by the antibiotic spectinomycin. <i>ACS Chem. Biol.</i> 2: 545-552
	2QBB	3.54	Borovinskaya, M.A., Pai, R.D., Zhang, W., Schuwirth, B.S., Holton, J.M., Hirokawa, G., Kaji, H., Kaji, A., Cate, J.H., (2007) <i>Nat. Struct. Mol. Biol.</i> 14: 727-732
	2QOY	3.50	Borovinskaya, M.A., Shoji, S., Holton, J.M., Fredrick, K., Cate, J.H., (2007) <i>ACS Chem. Biol.</i> 2: 545-552
	1VS5	3.46	Schuwirth, B.S., Day, J.M., Hau, C.W., Janssen, G.R., Dahlberg, A.E., Cate, J.H.D., Vila-Sanjurjo, A., (2006) <i>Nat. Struct. Mol. Biol.</i> 13: 879-886
<i>Tetrahymena thermophila</i>	2XZM	3.93	Rabl, J., Leibundgut, M., Ataide, S.F., Haag, A., Ban, N. (2011) <i>Science</i> 331 : 730-736

All the ribosomal proteins were analyzed in terms of sequence and three dimensional structural alignment, using PDBeFold server of EBI (<http://www.ebi.ac.uk/msd-srv/ssm/cgi-bin/ssmserver>). The root mean square deviation (RMSD) of two aligned protein structures in their three dimensional complexed conformation by SSM algorithm (RMSD of distances between C α -atoms of matched residues at best 3D superposition of the template and target structures) is defined as:

$$RMSD = \sqrt{Ga^2 + Gb^2 - 2 \frac{\sum_i Rai \cdot Rbi}{\sqrt{\sum_i Rai^2 \sum_i Rbi^2}} GaGb}$$

Where Ga and Gb are the radius of gyration for structures A and B, Rai and Rbi are the co-ordinate vectors of C α -atoms of proteins A and B after global superposition. Generally, the larger the RMSD, the distant the two matched structures are (Krissinel, 2004; Edger 2004). As suggested by Krissinel and Henrick in 2004 (Krissinel and Henrick, 2004), RMSD cannot be considered as a good measure of three dimensional structure dissimilarity when the target structure is a little distorted replica of the template (by a few Å), because the quality of alignment is often improved by unmapping the C α atoms of less similar parts. Usually this is achieved by introducing a cut-off distance of about 2-4Å in SSM algorithm. Only that structure alignment is considered to be of a good quality that provides minimum RMSD for an alignment of maximum number of residues (N_{align}). Therefore, a quality factor has been suggested to quantify numerically the quality of alignment (denoted by Q) and it is defined as:

$$Q = N_{align}^2 / [1 + (RMSD/R_0)^2] N_1 N_2$$

Here N_1 and N_2 are the number of residues present in template and target structures. R_0 is an empirical parameter (chosen at 3Å) that measures the relative significance of RMSD and N_{align} (Krissinel and Henrick, 2004). The Q-value is unity only for identical structures. The RMSD and Q-scores of 3D structural alignment were calculated for the multiple structural alignments of all corresponding ribosomal proteins for the 15 ribosomal complexes, using PDBeFold server. The amino acid sequence identity between the corresponding proteins was also analyzed quantitatively using the same server, where similarity between identical sequences is represented by unity. The more the identity factor is close to unity, the similar the two sequences are.

1.2 ANALYSIS OF PROTEIN-rRNA AND PROTEIN-PROTEIN INTERFACES

The structural characterization of protein-protein and protein-RNA interfaces were first conducted by Janin *et al.* in 1988, Miller in 1989, Argos in 1988 and Thornton and coworkers (Jones and Thornton, 1995, 1996; Jones *et al.*, 1999, 2001), which concentrated both on the protein-protein and protein-nucleic acid interfaces characterized in terms of hydrophobicity, accessible surface area, interface shape and residue propensities. The comparisons of different types of protein complexes (enzyme-inhibitor and antibody-antigen) in terms of interface size and hydrophobicity have been analyzed by Janin and coworkers (Janin and Chothia, 1990; Duquerroy *et al.*, 1991). Korn and Burnett in 1991, Young *et al.* in 1994 and Thornton *et al.* and coworkers have contributed progressively on the protein-protein interfaces thereafter. The researches on protein-nucleic acid interfaces started with some pioneer works of Steitz in 1990, Harrison in 1991 and Thornton and coworkers (Jones *et al.*, 1999; Luscombe *et al.*, 2000; Jones *et al.*, 2001), where they concentrated on the characterization of the corresponding interfaces. Olson and co-workers (Olson 19996; Olson and Zhurkin, 1996; Olson *et al.*, 1998) detected the DNA structures distort upon protein binding which was also supported by Dickerson in 1998. These works also have revealed the sequence

dependent nature of the protein-DNA binding sites. However, the protein-RNA interfaces have also been analyzed in detail, with the example of Thornton et al. in 2001.

In case of protein-protein contacts, an amino acid residue is defined as an interface residue if it loses $>1\text{\AA}^2$ of its accessible surface area when passing from uncomplexed state to complexed state (Jones et al., 1995). Jones et al. in 1999 and 2001 has shown that this is applicable to protein-RNA and protein-DNA complexes as well. By calculating the accessible surface area of the amino acid residues in the complexed three dimensional conformation both in complexed state (protein-RNA) and being isolated from the complex (only protein), it is possible to identify the amino acid residues with accessible surface area reduced $>1\text{\AA}^2$ on complex formation with ribosomal RNA. They are known as the interface residues and the total number of interface residues in a single protein defines its RNA binding site (Janin et al., 1998). The Surface Racer program (Tsodikov et al., 2002) was used to calculate the accessible and buried surface areas of the proteins and RNA, with probe radius taken to be 1.4\AA , which resembles the radius of one water molecule. We calculated the water accessible surface area (ASA) of the two interacting partners using Surface racer program separately (in their complexed conformation) and in associated state. If the ASA of the two partners are A1 and A2 and of their associated structure is A3, then buried surface area is

$$BSA = 1/2 \{(A1 + A2) - A3\}$$

These results were compared with those provided by PDBePisa (Krissinel and Henrick, 2005, 2007; Krissinel 2009) web server of EBI (URL: <http://ebi.ac.uk/msd-srv/prot-int/cgi-bin/piserver>).

The %polarity of any protein-protein or protein-nucleic acid interface is defined as:

$$\%Polarity = \frac{BSA(polar)}{BSA(protein)} \times 100$$

where BSA (polar) is the buried surface area of polar atoms and BSA (protein) is the buried surface area of the total protein due to complex formation. For each ribosomal protein, this equation was used to calculate the %polarity of its interface with 16S rRNA. We also calculated the data of solvation free energy of association of each ribosomal protein that indicate the thermodynamic stability of every protein-protein and protein-RNA interface from PDBePisa server (Krissinel and Henrick, 2005, 2007; Krissinel 2009), compiled, and presented accordingly.

1.3 ANALYSIS OF ATOM-ATOM CONTACTS

We focused on the main two kinds of atom-atom contacts stabilizing the protein-rRNA interfaces: hydrogen bonds and van der Waals contacts. Intermolecular hydrogen bonds were calculated for protein-RNA complexes using NCONT program of ccp4i program suite (Winn et al., 2011), Discovery Studio Visualizer program (Accelrys Software Inc.) and UCSF Chimera software (Pettersen et al., 2004). The theoretical criteria used to define a hydrogen bond was the D-A distance $\leq 3.35\text{\AA}$, and D-H-A angle to be within 90° - 180° , where D stand for the donor group and A for the acceptor group. The van der Waals contacts between protein and RNA were defined as all contacts between atoms excluding those involved in hydrogen bonds that are $\leq 4.0\text{\AA}$ apart (Jones et al., 2001). Distance criteria for van der Waals contact within protein are taken to be $\leq 5.0\text{\AA}$. The hydrogen bonding and van der Waals contact information was also calculated from the PDBePisa server (Krissinel and Henrick, 2005, 2007; Krissinel 2009) of EBI for all 15 ribosomal complexes, and were compared with Discovery Studio Visualizer and UCSF Chimera output. For each ribosomal protein, the surface density of Hydrogen bonding, defined as the number of hydrogen bonds per 100\AA^2 buried surface area due to complex formation, was calculated from the available data, both at its RNA and protein-binding sites. All the data were compiled and presented according to the classifications adopted for the ribosomal proteins.

1.4 PROTEIN CONFORMATIONAL CHANGES DUE TO COMPLEX FORMATION

Binding of proteins with other proteins or nucleic acids is usually accompanied by significant changes of their three-dimensional conformations. There are prior works that predicted that there is a relationship between the conformational changes a protein undergoes upon complex formation and the interface size of the resulting complex. Janin et al. (4) predicted that complexes with large interfaces must require major structural changes upon complex formation due to the excessive accessible surface of their isolated subunits. Lo Conte et al. in 1999) showed that the subunits of protein complexes with large interfaces ($BSA > 2000\text{\AA}^2$) tend to undergo

greater conformational changes upon complex formation, compared to those with smaller interfaces. The connection between the intrinsic flexibility of unbound proteins and the conformations they adopt upon binding has been analyzed in detail by Marsh and Teichmann in 2011. Analyzing accessible surface area of 4988 monomeric proteins Marsh and Teichmann were able to find out a relationship between molecular weight (M) and accessible surface area for all monomers:

$$ASA = 4.84M^{0.760}$$

Since this equation is highly predictive of the ASA of monomeric and folded proteins, the authors concluded that the deviation of ASA from its predicted value might be a useful indicator of to what extent a protein resembles a folded monomer. They defined relative solvent accessible surface area, denoted by $ASA(rel)$ as observed ASA scaled by its predicted value from the molecular weight:

$$ASA(rel) = \frac{ASA(observed)}{ASA(predicted)}$$

The $ASA(rel)$ value for each subunit is to be considered in its bound conformation, isolated from the rest of the complex. By plotting the $ASA(rel)$ with RMSD values of complexed and uncomplexed conformations, the authors have observed the following relationships:

$$RMSD(homomer) = \exp [6.14 \times ASA(rel)^{complexed} - 5.95]$$

$$RMSD(heteromer) = \exp [6.35 \times ASA(rel)^{complexed} - 6.05]$$

Applying this algorithm proposed by Teichmann et al., we have tried to predict the three dimensional conformational changes of all the r-proteins due to their transition from the complexed state to the uncomplexed state. Since ribosomal proteins are all heteromers, the second equation will tell us the RMSD values between the complexed and uncomplexed states of each ribosomal protein. The ASA of the ribosomal proteins in their complexed conformation isolated from ribosomal assembly were calculated using Surface Racer program (22), and exact molecular weights were calculated using Discovery Studio Visualizer software (27). All the available data were compiled according to the classifications of r-proteins we adopted.

The Marsh and Teichmann algorithm we applied here describes a strategy to predict whether a protein structure is intrinsically disordered or not. The $ASA(rel)$ value of one monomer in bound state being ≥ 1.2 indicates a structurally flexible protein; whereas a value ≥ 1.4 indicates an intrinsically disordered protein structure.

1.5 ANALYSIS OF SEQUENCE CONSERVATION AT THE BINDING SITE

We are interested about the extent of amino acid sequence conservation of the binding sites of the ribosomal proteins, compared to that of the rest of protein surface. The conservation of the sequences at the binding sites since conservation of sequences or their substitution by residues of same chemical property is necessary for structural integrity. Taking under consideration 20 bacterial species from the bacterial phylogeny and of diverse availability in nature, we have tried to analyze the degree of conservation of the amino acid residues at the binding sites. The 20 species are *Escherichia coli*, *Vibrio cholerae*, *Staphylococcus aureus*, *Thermus thermophilus*, *Salmonella enterica*, *Micobacterium tuberculosis*, *Helicobacter pylori*, *Mycoplasma crocodyli*, *Actinobacter baumannii*, *Agrobacterium radiobacter*, *Cellulophaga lytica*, *Streptococcus pneumoniae*, *Persephonella marina*, *Nitrobacter hamburgensis*, *Pseudomonas putida*, *Rhodospirillum rubrum*, *Anabaena variabilis*, *Caulobacter crescentus*, *Chlorobium luteolum*, and *Actinomyces oris*. They contain a large variety of archaea, proteobacteria, firmicutes, actinobacteria, and modern bacteria, with observable diversity in availability in nature as well. The sequences of all the ribosomal proteins for these 20 bacterial species were collected from NCBI and using MUSCLE multiple sequence alignment program (Edgar, 2004) they were aligned together. The aligned sequences were then represented graphically as sequence logos using WebLogo server (Crooks et al., 2004) according to the probability of occurrence of them in the 20 different species. This gives us a visualized demonstration of the sequence similarity, conservation and the replacement of various amino acid residues throughout the evolution. In the WebLogo output, the sequences corresponding to *E. coli* that take part in the interactions (protein-protein and protein-RNA) were marked with information about both the van der Waals and Hydrogen bonding contacts at the binding sites.

To compute numerically the conservation of residues at the binding sites, we are proposing a new parameter: “the binding site residue conservation factor,” denoted by C_T , which is defined as:

$$C_T = \frac{N_C^B/N^B}{N_C^S/N^S}$$

where, N_C^B is the number of amino acid residues at the interfaces that are conserved to a cutoff value denoted by T, normally expressed in percentage of conservation (e.g. 70% cutoff conservation, T=70%). N^B is the total number of interface residues; N_C^S is the number of amino acid residues at the protein surface excluding binding sites that are conserved to a cutoff value denoted by T and N^S is the total number of surface residues excluding interface. The residue conservation factor being >1 , we can say that the corresponding protein shows higher tendency in preserving the amino acid sequences at the binding sites, compared to the rest of its surface residues. Varying the cutoff value of conservation from 50% to 100% at a step of 10%, we have calculated C_T in each case.

The binding site of proteins does not only contain all the conserved residues, but there are many residues (identified for *E. coli*) that have been replaced by other residues in other bacterial species. We have observed that the substitutions of the residues at the binding sites follow a distinct pattern: there is a slight higher tendency of substituting the residues by those of similar charge (positive-to-positive, negative-to-negative, and neutral-to-neutral) at any given position compared to rest parts of the proteins (discussed in detail in Results and Discussions). To verify this, we are proposing another factor, the “interface charge conservation factor,” denoted by P_c as:

$$P_c = \frac{N_C^B/N_T^B}{N_C^S/N_T^S}$$

where N_C^B is the number of replacements of the amino acid residues by those of the same charge (positive-to-positive, negative-to-negative, neutral-to-neutral), plus the number of conserved residues at the interface. N_T^B is the total number of replacements of all residues at the interface, N_C^S is the number of the residues replaced by those of the same charge, plus the number of conserved residues at the protein surface excluding interface and N_T^S is the number of replacement of all residues at the surface excluding interface. At any given position at the binding site, if one residue is conserved, or is substituted by other residues of same charge, then we can say that the residue positional charge is conserve there. The interface residue conservation factor computationally measures the higher tendency of conserving the residue positional charge at the interface, compared to rest of the protein surface, if its numerical value is >1 . In this algorithm, it is considered that one amino acid has been replaced by others of same charge if the probability of occurrence of all residues of the same charge at that position is $\geq 90\%$, or is conserved if its probability of occurrence at that position is $\geq 90\%$.

1.6 STATISTICAL TESTS AND CALCULATIONS

1.6.1 DATA CLUSTERING

The protein-RNA and protein-protein interface properties were clustered together to find out the high importance of a group of proteins over the others in ribosomal stabilization. Simple Hierarchical clustering algorithms (Gronau and Moran, 2007) were used in our analysis to identify groups of proteins with some unique interface features. Globally closest pair clustering algorithms was tested on our data samples and simple UPGMA (Unweighted Pair Grouping Method with Arithmetic mean) is selected for all the analysis. In this method, the input is a dissimilarity matrix D over a set of elements S .

Initialization: A cluster set C is initialized by defining a singleton cluster $C_i = \{i\}$ for every element $i \in S$. Output hierarchy is initialized $H \leftarrow C$.

Loop: While $|C| > 1$, the following steps are accepted:

1. Cluster pair selection: A pair of distinct clusters is selected $\{C_i, C_j\} \subseteq C$ of minimum dissimilarity under D .

2. Cluster pair joining: C_i, C_j are removed from the cluster set C and is replaced by $C_i \cup C_j$. $C_i \cup C_j$ cluster is then added to the hierarchy H .
3. The dissimilarity $D(C_k, (C_i \cup C_j))$ for every $C_k \in C' \setminus (C_i \cup C_j)$ is calculated.

Finalize: Return to the hierarchy H .

The dissimilarity matrix in UPGMA method defines the dissimilarity between clusters as their average dissimilarity. This is achieved by using the following reduction formula (ref. 36):

$$D(C_k, (C_i \cup C_j)) \leftarrow \frac{|C_i|}{|C_i| + |C_j|} D(C_k, C_i) + \frac{|C_j|}{|C_i| + |C_j|} D(C_k, C_j)$$

The commutativity property holds trivially when the reduction formula F induces a dissimilarity function D_F over the set of all clusters, s.t. $D_F(C_1, C_2)$ depends only on the dissimilarities between elements in $C_1 \cup C_2$. Such are for instance the reduction formulae for UPGMA (ref. 32):

$$D_{UPGMA}(C, C') = \frac{1}{|C||C'|} \sum_{i \in C, j \in C'} D(i, j)$$

So, utilizing UPGMA clustering method, groups of proteins sharing common features are identified. This enables us to identify the roles of different groups of proteins in structural assembly.

1.6.2 MANN-WHITNEY U-TESTS

Uniqueness (in terms of structural features) of each of the protein groups were statistically tested in terms of Mann-Whitney U-test for comparison (Mann and Whitney, 1947). The null hypothesis adopted: the two groups of data selected for analysis originate from the same population. The alternate hypothesis is: the two sets of data selected for analysis originate from two different populations. The null hypothesis is rejected and the alternate hypothesis is accepted when $p \leq 0.01$. When $0.01 < p < 0.05$, we concluded that the two sets of data are marginally different (different populations). The two groups of data are considered to be originated from the same population, if $p \geq 0.05$.

All the clustering algorithms and U-tests were carried on using PAST statistical software package (Hammer et al., 2001). In this work, we also have tried to correlate some interface parameters, the correlation coefficients of whom were also calculated using PAST. The statistics of various linear and surface fitting were calculated using Origin data analysis and graphic workspace (OriginLab Corporation). Origin was also used to produce graph plots included in this supplementary material.

2. RESULTS AND DISCUSSION

2.1 RESULTS

Table S2: The classifications of the ribosomal proteins of *E. coli* and *T. thermophilus* according to their association with the 16S RNA and according to their individual influence in structure stabilization.

Ribosomal protein classifications according to their association with the complex		Ribosomal protein classifications according to their influence in 30S structure stabilization	
Classifications	Proteins	Classifications	Proteins
Primary Binders	S4, S7, S8, S15, S17 & S20	Group-1	S4, S9, S12
Secondary Binders	S9, S12, S13, S16, S18 & S19	Group-2	S16, S17, S20
Tertiary Binders	S2, S3, S5, S6, S10, S11, S14, S21 & THX	Group-3	S3, S5, S7, S8, S10, S11, S13, S14, S15, S19
		Group-4	S2, S6, S18, S21, THX

Table S3: The buried surface area of the ribosomal proteins for *Thermus thermophilus* and *Escherichia coli*.

Ribosomal proteins	Average BSA of <i>T. thermophilus</i> proteins (Å ²)	Standard Deviation	BSA of <i>E. coli</i> proteins (Å ²)	Standard deviation
S2	998.71	74.43	937.12	88.90
S3	1691.35	56.04	1622.40	86.32
S4	2965.99	243.30	3006.92	93.88
S5	1959.26	53.15	1769.82	54.93
S6	647.18	189.11	432.66	30.73
S7	1859.82	76.37	1790.46	84.70
S8	1874.48	77.83	1742.46	24.97
S9	2943.62	173.86	2836.02	43.67
S10	1801.79	40.92	1742.60	27.61
S11	1825.82	31.41	2000.72	6.52
S12	3106.87	118.09	2751.24	151.00
S13	2155.44	128.88	1808.47	49.70
S14	1931.28	99.15	2072.64	101.79
S15	1776.25	36.98	1628.04	36.62
S16	2505.85	69.35	2099.58	53.48
S17	2669.90	72.11	1603.21	37.27
S18	864.57	14.37	935.93	40.09
S19	1549.82	162.29	1550.89	91.95
S20	2541.10	88.14	2139.38	47.71
S21	-	-	514.84	36.25
THX	1287.49	34.63	-	-

Table S4: The free energy of association of the ribosomal proteins with 16S rRNA for *Thermus thermophilus* and *Escherichia coli*.

Ribosomal proteins	Solvent free energy of association (ΔG) with 16S rRNA (Kcal/mole) for <i>T. thermophilus</i> proteins	Standard Deviation	Solvent free energy of association (ΔG) with 16S rRNA (Kcal/mole) for <i>E. coli</i> proteins (Å ²)	Standard deviation
S2	-17.58	4.17	-19.28	2.68
S3	-28.49	1.79	-32.68	0.85
S4	-52.60	2.36	-61.79	3.75

S5	-33.96	1.56	-30.32	0.97
S6	-8.18	0.30	-8.10	0.62
S7	-25.05	3.47	-26.26	6.02
S8	-28.46	0.75	-28.06	1.93
S9	-54.36	2.20	-51.54	4.52
S10	-28.37	3.05	-26.65	2.14
S11	-32.58	0.84	-34.22	1.45
S12	-58.13	1.40	-50.99	1.85
S13	-42.98	4.91	-42.38	0.75
S14	-31.68	3.57	-41.24	2.61
S15	-37.01	1.67	-29.98	2.27
S16	-45.88	4.38	-37.11	2.35
S17	-42.38	2.03	-33.09	1.36
S18	-20.17	0.63	-19.02	1.46
S19	-19.01	3.26	-19.10	3.58
S20	-51.56	1.52	-44.66	1.64
S21	-	-	-9.80	2.06
THX	-27.09	3.17	-	-

Table S5: Mann-Whitney U-test results. In this table, the average values of the physical parameters between the two bacterial species (*T. thermophilus* and *E. coli*) are used for each protein of the groups.

Interface Properties	U-test between groups	p-value	Two groups are from same/different populations
Buried Surface Area	Group-1 vs. Group-2	0.0994	Same population
	Group-2 vs. Group-3	0.00699	Different populations
	Group-3 vs. Group-4	0.000666	Different populations
	Group-4 vs. Group-1	0.03572	Different populations, difference is marginally significant
	Group-1 vs. Group-3	0.006993	Different populations
	Group-2 vs. Group-4	0.03571	Different populations, difference is marginally significant
	Primary vs. Secondary	0.9048	Same populations
	Secondary vs. tertiary	0.2571	Same populations
	Tertiary vs. Primary	0.04262	Different populations, difference is marginally significant
Primary and secondary vs. tertiary	0.03142	Different populations, difference is marginally significant	
Free energy of association with 16S rRNA	Group-1 vs. group-2	0.1	Same population
	Group-2 vs. Group-3	0.02797	Different populations, difference is marginally significant
	Group-3 vs. Group-4	0.002664	Different populations
	Group-4 vs. Group-1	0.03571	Different populations, difference is marginally significant
	Group-1 vs. group-3	0.006993	Different populations
	Group-2 vs. Group-4	0.03571	Different populations, difference is marginally significant
	Primary vs. Secondary	0.7302	Same populations
	Secondary vs. tertiary	0.1714	Same populations
	Tertiary vs. Primary	0.08125	Same populations
Primary and secondary vs. tertiary	0.04734	Different populations, difference is marginally significant	

Table S6: The free energy of association, Surface density of Hydrogen bond and van der Waals contacts at protein-rRNA interface of ribosomal proteins are displayed. The proteins are classified into four distinct groups according to importance in ribosomal structure stabilization. From this table, it is clear that Group-1 proteins are most important is stabilization of ribosomal complex with highest free energy of association and highest surface density of atomic contacts. Group-4 proteins are least important.

Protein Groups	Solvent free energy of association (ΔG) with 16S rRNA (Kcal/mole)	Average BSA of ribosomal proteins at rRNA interfaces (\AA^2)
----------------	---	---

Group-1	-54.90 (2.14)	2935.11 (48.60)
Group-2	-42.45 (5.25)	2259.84 (108.40)
Group-3	-30.92 (6.42)	1807.69 (143.05)
Group-4	-15.77 (7.73)	842.08 (322.49)

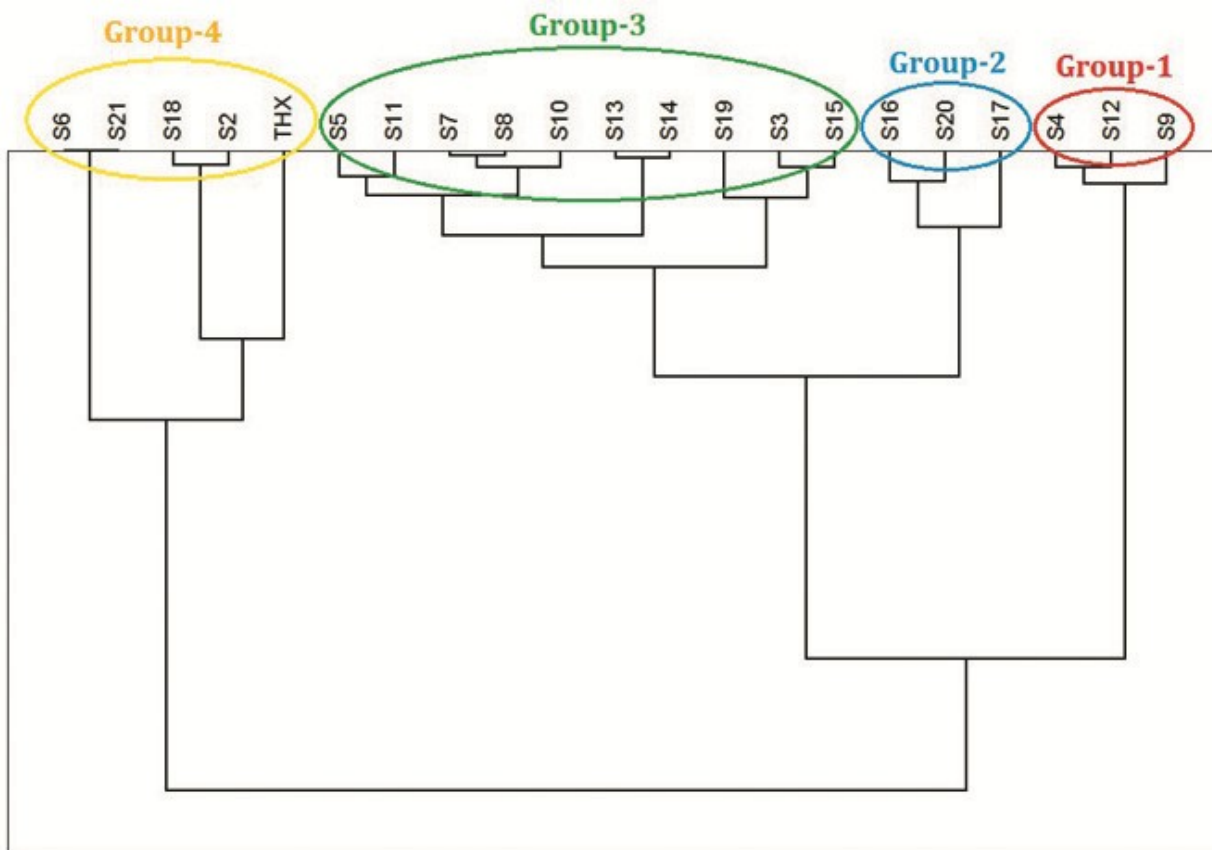


Figure F1: The dendrogram of the BSA-based clustering of the small-subunit ribosomal proteins using UPGMA method. Proteins of the Group-1 and Group-2 have the largest interface areas with 16S rRNA. Proteins of Group-4 have minimum interface areas. Proteins of Group-3 have moderately large interface areas. The image is produced by using PAST statistical software package (34).

Table S7: The protein-protein interface properties of the 30S ribosomal subunit. We can see that the available protein-protein interfaces are different for *T. thermophilus* and *E. coli*. From this table, we also observe that some of the smallest protein-protein interfaces do not contain Hydrogen bonds. For example, S2-S5 interface in *E. coli* do not contain any Hydrogen bonding.

Protein-protein interfaces	Buried surface area at the interface (Å ²)		Free energy of interface formation (Kcal/mole)		Surface Density of Hydrogen bonds (No. of bonds per 100 Å ² BSA)		Surface Density of van der Waals contacts (No. of contacts per 100 Å ² BSA)	
	<i>T. thermophilus</i>	<i>E. coli</i>	<i>T. thermophilus</i>	<i>E. coli</i>	<i>T. thermophilus</i>	<i>E. coli</i>	<i>T. thermophilus</i>	<i>E. coli</i>
S2-S3	56.3	-	1.2	-	2.1	-	6.3	-
S2-S5	65.6	29.5	1.1	0.7	-	-	6.1	3.6
S2-S8	258.7	2.9	-0.9	0.1	1.3	-	13.4	
S3-S4	37.4	20.0	0.8	0.6	5.2	-	11.6	3.8
S3-S5	77.2	145.2	0.7	1.1	1.3	1.3	6.3	5.8
S3-S10	396.1	326.5	-3.5	-4.7	0.5	0.5	10.9	6.7
S3-S14	831.6	883.7	-8.8	-9.1	0.6	0.9	10.4	13.4
S4-S5	354.0	264.2	0.6	-0.8	0.8	0.8	5.9	11.3
S5-S8	566.9	487.2	-1.6	-4.0	1.0	0.7	11.7	12.5
S6-S18	1027.5	669.9	-8.2	-6.9	35.7		15.6	
S7-S9	251.7	92.6	-3.6	-0.8	0.2	0.2	6.0	0.7
S7-S11	234.3	182.9	-1.3	-1.9	0.6	3.3	9.2	19.3
S8-S12	57.9	58.0	-1.0	-0.7	0.0		4.7	0.8
S8-S17	125.2	122.0	-0.5	-0.9	1.7	3.5	8.2	18.1
S9-S10	160.0	137.2	-0.6	-0.9	0.8	0.8	9.1	4.3
S9-S13	68.1	76.9	0.1	0.4	0.9	0.7	11.1	10.0
S9-S14	809.4	763.8	-8.2	-8.0	2.0		6.3	
S10-S14	311.4	122.6	-1.0	0.3	8.9	2.1	14.3	10.1
S11-S18	207.2	196.1	-3.3	-3.2	0.6	0.1	12.1	2.5
S12-S17	402.9	364.3	-3.5	-2.0	0.3	2.0	5.8	30.9
S13-S19	-	988.9	-	-6.0	1.0	7.8	6.6	80.8
S11-S21	-	248.0	-	-2.3	-	0.5	-	3.5

Table S8a: The A_{REL} values (expressing the structural flexibility of proteins) of small subunit ribosomal proteins are enlisted here. Data are calculated according to Marsh and Teichmann algorithm (section 1.4). The $A_{REL}>1.2$ indicated structural flexibility and $A_{REL}>1.4$ indicates intrinsic disorder of corresponding proteins. Averaging between two species, we see S14 is intrinsically disordered, and S12, S13 has a very high structural flexibility. On the other hand, S2, S6, S16 are structurally very rigid proteins.

Ribosomal proteins	A_{REL} values for <i>T. thermophilus</i>	Standard Deviation	A_{REL} values for <i>E. coli</i>	Standard deviation	Average A_{REL}
S2	1.10	0.04	1.12	0.05	1.11
S3	1.20	0.03	1.22	0.05	1.22
S4	1.16	0.02	1.19	0.05	1.17
S5	1.12	0.03	1.12	0.03	1.12
S6	1.03	0.03	1.16	0.05	1.10
S7	1.22	0.05	1.27	0.04	1.25
S8	1.10	0.02	1.12	0.04	1.11
S9	1.21	0.02	1.24	0.05	1.23
S10	1.27	0.02	1.29	0.05	1.28
S11	1.20	0.02	1.22	0.03	1.21
S12	1.33	0.03	1.41	0.05	1.37
S13	1.28	0.03	1.36	0.06	1.32
S14	1.40	0.03	1.41	0.04	1.41
S15	1.17	0.01	1.22	0.06	1.20
S16	1.13	0.01	1.08	0.04	1.11
S17	1.21	0.02	1.30	0.05	1.26
S18	1.14	0.03	1.20	0.04	1.17
S19	1.20	0.02	1.25	0.05	1.23
S20	1.23	0.01	1.23	0.22	1.23

S21	-	-	1.18	0.04	1.18
THX	1.49	0.06	-	-	1.49

Table S8b: The constant terms (a, b and c) and the surface fitting statistics of three parameters of ribosomal proteins: Free energy of association, Buried surface area and RMSD between complexed and uncomplexed states. Predicted equation is: $\Delta G = a + b(BSA) + c(RMSD)$

Constant terms	<i>Thermus thermophilus</i>	<i>Escherichia coli</i>	<i>Tetrahymena thermophila</i>
a	2.099	4.421	-2.259
b	-0.009	-0.231	-0.018
c	-0.019	-0.019	0.257
R-value of surface fitting	0.95	0.94	0.93
R-square value of surface fitting	0.89	0.89	0.86

Table S9a: The residue conservation factor and charge conservation factor for ribosomal proteins classified according to association at different conservation cutoffs.

Residue Conservation factor according to protein classification (at various conservation cutoffs)							Charge Conservation factor
Protein Classifications	50% conservation	60% conservation	70% conservation	80% conservation	90% conservation	100% conservation	
Primary	1.20	1.32	1.48	1.56	1.65	2.01	1.36
Secondary	1.26	1.37	1.44	1.51	1.76	2.07	1.30
Tertiary	1.30	1.42	1.45	1.57	2.05	3.79	1.32

Table S9b: The residue conservation factor for ribosomal proteins at different conservation cutoffs.

Ribosomal Proteins	Residue conservation factor (various cutoffs)						Charge conservation factor
	50% conservation	60% conservation	70% conservation	80% conservation	90% conservation	100% conservation	
S2	1.71	2.05	2.01	2.67	3.14	4.47	2.49
S3	1.14	1.25	1.38	1.44	1.43	2.44	1.57
S4	1.08	1.24	1.22	1.41	1.63	2.49	1.52
S5	1.29	1.31	1.64	1.75	1.77	3.62	1.14
S6	1.71	1.66	1.97	1.71	3.41	8.53	1.39
S7	0.99	1.04	1.07	1.04	0.85	0.55	0.92
S8	1.38	1.38	1.42	1.91	2.79	3.12	1.40
S9	1.48	1.84	1.97	1.85	1.89	1.86	1.63
S10	1.41	1.61	1.46	1.67	1.75	3.38	1.17
S11	1.10	1.32	1.40	1.64	1.65	1.72	1.03
S12	1.07	1.04	1.04	1.02	1.11	1.15	1.01
S13	1.61	1.75	1.97	2.18	2.24	2.56	1.84

S14	0.99	1.15	1.11	1.11	1.21	2.38	0.97
S15	1.49	1.61	1.99	1.83	1.96	2.74	1.77
S16	1.05	1.12	1.24	1.60	2.42	2.23	1.07
S17	1.08	1.06	1.21	1.09	1.02	1.13	1.09
S18	1.29	1.24	1.17	1.08	1.36	3.09	0.89
S19	1.06	1.22	1.26	1.33	1.53	1.53	1.38
S20	1.17	1.61	1.97	2.07	-	-	1.46
S21	1.04	1.04	0.63	0.56	-	-	0.81

Large proteins like S3, S4, S5 and S6 also show high binding site residue conservation factor. However, there is almost no correlation identified between the conservation tendency and protein size, association or architecture.

Table S10: The surface density of Hydrogen bonds at the protein-rRNA interfaces of *Thermus thermophilus* and *Escherichia coli* ribosomes.

Ribosomal proteins	Surface Density of H-bonds ($\sigma(H)$) at protein-rRNA interface (No. of bonds per 100Å ² BSA) for <i>T. thermophilus</i> proteins	Standard Deviation	Surface Density of H-bonds ($\sigma(H)$) at protein-rRNA interface (No. of bonds per 100Å ² BSA) for <i>E. coli</i> proteins (Å ²)	Standard deviation
S2	1.24	0.41	1.31	0.48
S3	1.74	0.34	1.72	0.41
S4	2.32	0.38	1.80	0.26
S5	2.09	0.24	1.78	0.42
S6	2.17	0.44	1.26	0.50
S7	2.37	0.53	1.74	0.38
S8	1.81	0.28	1.98	0.16
S9	2.28	0.61	2.20	0.29
S10	1.44	0.34	1.63	0.20
S11	1.93	0.29	1.80	0.26
S12	2.21	0.33	2.17	0.27
S13	2.20	0.40	2.21	0.34
S14	1.71	0.44	2.34	0.31
S15	1.65	0.30	1.67	0.35
S16	1.73	0.18	1.67	0.15
S17	1.95	0.29	1.74	0.25
S18	2.00	0.28	2.39	0.28
S19	1.91	0.26	1.92	0.39
S20	1.98	0.36	1.68	0.39
S21	-	-	0.82	0.33
THX	2.14	0.36	-	-

Table S11: The surface density of van der Waals contacts at the protein-rRNA interfaces of *Thermus thermophilus* and *Escherichia coli* ribosomes.

Ribosomal proteins	Surface Density of van der Waals contacts ($\sigma(v)$) at protein-rRNA interface (No. of bonds per 100Å ² BSA) for <i>T. thermophilus</i> proteins	Standard Deviation	Surface Density of van der Waals contacts ($\sigma(v)$) at protein-rRNA interface (No. of bonds per 100Å ² BSA) for <i>E. coli</i> proteins (Å ²)	Standard deviation
S2	12.6	1.2	10.9	1.8
S3	16.8	0.9	16.8	1.2
S4	15.3	1.3	14.7	0.5

S5	14.4	0.8	15.6	1.2
S6	14.4	1.5	9.0	2.2
S7	19.1	1.4	15.7	1.4
S8	14.9	0.9	17.0	1.2
S9	18.7	1.2	16.7	1.2
S10	15.9	0.8	14.6	0.8
S11	17.4	1.5	17.3	0.6
S12	15.8	0.8	16.1	0.8
S13	19.4	1.9	18.9	2.1
S14	15.2	1.9	16.0	0.2
S15	15.6	1.0	15.3	1.4
S16	13.6	0.7	12.7	0.4
S17	16.6	1.7	13.8	1.4
S18	13.8	0.8	16.2	2.5
S19	19.7	1.0	19.7	1.6
S20	16.1	0.8	13.8	0.7
S21	-	-	10.3	2.9
THX	13.7	0.8	-	-

Table S12: The Base/Backbone ratio and the %polarity data of the ribosomal proteins for *T. thermophilus* and *E. coli*.

Ribosomal Proteins	Interface Polarity		Base/backbone ratio	
	<i>T. thermophilus</i>	<i>E. coli</i>	<i>T. thermophilus</i>	<i>E. coli</i>
S2	65.12	62.04	0.97	0.69
S3	61.53	60.31	0.91	0.81
S4	68.30	62.59	0.39	0.49
S5	63.32	60.01	0.73	0.96
S6	62.70	59.95	0.34	0.37
S7	68.78	57.30	0.74	1.32
S8	54.88	59.09	1.77	2.27
S9	66.45	59.77	0.35	0.40
S10	59.15	59.07	0.73	0.79
S11	64.37	62.27	0.80	1.08
S12	68.39	70.04	0.42	0.59
S13	65.23	65.19	0.43	0.15
S14	67.38	64.30	0.46	0.46
S15	61.58	64.17	1.07	2.02
S16	62.59	62.04	0.57	0.50
S17	62.92	61.37	0.81	0.85
S18	63.20	61.90	0.81	0.87
S19	59.72	63.99	1.82	0.84
S20	68.99	68.69	0.78	0.35
THX	-	66.98	-	0.75
S21	67.97	-	0.13	

3. REFERENCES

Argos, P. (1988). An investigation of protein subunit and domain interfaces. *Protein Eng.* 2, 101-113.

Crooks, G. E., Hon, G., Chandonia, J., Brenner, S. E. (2004). WebLogo: a sequence logo generator. *Genome Research*; 14:1188–1190.

Dickerson, R.E. (1998). DNA bending: the prevalence of kinkiness and the virtues of naormality. *Nucleic Acids Research*, 1998, Vol. 26, No. 8, 1906–1926.

Discovery Studio Visualizer, Copyright ©2010, Accelrys Software Inc. All rights reserved.

Duquerroy, S., Cherfils, J. and Janin, J. (1991). Protein-protein interaction: an analysis by computer simulation. *Ciba Found. Symp.* 161, 237-252.

Edgar, R. C. (2004), MUSCLE: multiple sequence alignment with high accuracy and high throughput, *Nucleic Acids Research* 32(5), 1792-97.

Gronau, I., Moran, S. (2007) Optimal Implementations of UPGMA and Other Common Clustering Algorithms. *Information Processing Letters*, Volume 104 Issue 6, Pages 205-210.

Hammer Ø., Harper, D. A. T., and Ryan, P. D. (2001). PAST: Paleontological Statistics software package for education and data analysis. *Paleontological Electronica* 4(1): 9pp. Version 2.10 used.

Harrison, S.C. (1991). A structural taxonomy of DNA-binding domains. *Nature*, 353, 715-719.

Janin J., Miller S., Chothia C. (1988) Surface, subunit interfaces and interior of oligomeric proteins. *J. Mol. Biol.* 204, 155–164.

Janin, J. and Chothia, C. (1990) The structure of protein-protein recognition sites. *J. Biol. Chem.* 265, 16027-16030.

Jones, S., Daley, D.T.A., Luscombe, N.M., Berman, H.M., Thornton, J.M. (2001). Protein-RNA interactions: a structural analysis. *Nucleic Acid research*, vol. 29, no. 4, 943-954.

Jones, S., Heyningen, P.V., Berman, H.M., Thornton, J.M. (1999) Protein-DNA interactions: a structural analysis. *J. Mol. Biol.* 287, 877-896.

Jones, S., Thornton, J.M. (1995). Protein-protein interactions: a review of protein dimer structures. *Prog. Biophys. Mol. Biol.* 63, 31-65.

Jones, S., Thornton, J.M. (1996). Principles of protein-protein interactions. *Proc. Natl. Acad. Sci. USA.* 93, 13-20.

Korn, A. P. and Burnett, R. M. (1991). Distribution and complementarity of hydrophathy in multi-subunit proteins. *Proteins: Struct. Funct. Genet.* 9, 37-55.

Krissinel, E. (2009). Crystal contacts as nature's docking solutions. *J Comput Chem.* 2010 Jan 15;31(1):133-43.; DOI 10.1002/jcc.21303

Krissinel, E. B., Winn, M. D., Ballard, C. C., Ashton, A. W., Patel, P., Potterton, E. A., McNicholas, S. J., Cowtan, K. D., Emsley, P. (2004). The new CCP4 coordinate library as a toolkit for the design of coordinate related applications in protein crystallography. *Acta Cryst. D60*, 2250–2255.

Krissinel, E., Henrick, K. (2004). Secondary structure matching (SSM), a new tool for fast protein structure alignment in three dimensions. *Acta Cryst.. D60*, 2256-2268.

Krissinel, E., Henrick, K. (2005). Detection of Protein Assemblies in Crystals. In: M.R. Berthold et.al. (Eds.): *CompLife*, LNBI 3695, pp. 163--174. Springer-Verlag Berlin Heidelberg.

Krissinel, E., Henrick, K. (2007). Inference of macromolecular assemblies from crystalline state. *J. Mol. Biol.* 372, 774--797.

Lo Conte L. Chothia C. Janin J. (1999) The atomic structure of protein-protein recognition sites. *J. Mol. Biol.* 285,2177–2198.

Luscombe, N.M., Austin, S.E., Berman, H.M. and Thornton, J.M. (2000). An overview of the structures of protein-DNA complexes. *Genome Biol.* 1, 1-37.

Mann, H. B.; Whitney, D. R. (1947). On a Test of Whether one of Two Random Variables is Stochastically Larger than the Other. *Annals of Mathematical Statistics* 18 (1): 50–60. doi:10.1214/aoms/1177730491. MR22058. Zbl 0041.26103.

Marsh, J.A., Teichmann, S.A. (2011). Protein solvent accessible surface area predicts protein conformational changes upon binding. *Structure.* 2011 June 08, 19(6), 859–867.

Miller S. (1989). The structure of interfaces between subunits of dimeric and tetrameric proteins. *Protein Eng.* 3, 77-83.

Olson, W. K. (1996). Simulating DNA at low resolution. *Curr. Opin. Struct. Biol.* 6, 242-256.

Olson, W. K. and Zhurkin, V. B. (1996). Twenty years of DNA bending. In *Ninth Conversation in Biomolecular Stereodynamics*, Adenine Press, Albany, NY.

Olson, W. K., Gorin, A. A., Lu, X. J., Hock, L. M. and Zhurkin, V. B. (1998). DNA sequence-dependent deformability deduced from protein-DNA crystal complexes. *Proc. Natl Acad. Sci. USA*, 95, 11163-11168.

OriginPro 8 SR0, v8.0724 (B724). Copyright © 1991-2007 OriginLab Corporation.

Pettersen, E.F., Goddard, T.D., Huang, C.C., Couch, G.S., Greenblatt, D.M., Meng, E.C., and Ferrin, T.E. (2004). UCSF Chimera - A Visualization System for Exploratory Research and Analysis. *J. Comput. Chem.* 25:1605-1612.

Steitz, T.A. (1990). Structural studies of protein-nucleic acid interaction: the source of sequence specific binding. *Q. Rev. Biophys.*, 23, 205-210.

Tsodikov, O. V., Record, M. T. Jr. and Sergeev, Y. V. (2002). A novel computer program for fast exact calculation of accessible and molecular surface areas and average surface curvature. *J. Comput. Chem.*, 23, 600-609.

Winn, M. D., Ballard, C. C., Cowtan, K. D., Dodson, E. J., Emsley, P., Evans, P. R., Keegan, R. M., Krissinel, E. B., Leslie, A. G. W., McCoy, A., McNicholas, S. J., Murshudov, G. N., Pannu, N. S., Potterton, E. A., Powell, H. R., Read, R. J., Vagin, A. and Wilson, K. S. (2011). Overview of the CCP4 suite and current developments. *Acta Cryst. D* 67, 235-242.

Young, L., Jernigan, R. L. and Covell, D. G. (1994). A role for surface hydrophobicity in protein-protein recognition. *Protein Sci.* 3, 717-729.